

A Tightly Coupled Bi-Level Coordination Framework for CAVs at Road Intersections

Donglin Li, Tingting Zhang *Member, IEEE*, Jiping Luo, Tianhao Liang, Bin Cao *Member, IEEE*, Xuanli Wu *Member, IEEE* and Qinyu Zhang *Senior Member, IEEE*

Abstract—Since the traffic administration at road intersections determines the capacity bottleneck of modern transportation systems, intelligent cooperative coordination for connected autonomous vehicles (CAVs) has shown to be an effective solution. In this paper, we try to formulate a Bi-Level CAV intersection coordination framework, where coordinators from High and Low levels are tightly coupled. In the High-Level coordinator where vehicles from multiple roads are involved, we take various metrics including throughput, safety, fairness and comfort into consideration. Motivated by the time consuming space-time resource allocation framework in [1], we try to give a low complexity solution by transforming the complicated original problem into a sequential linear programming one. Based on the “feasible tunnels” (FT) generated from the High-Level coordinator, we then propose a rapid gradient-based trajectory optimization strategy in the Low-Level planner, to effectively avoid collisions beyond High-level considerations, such as the pedestrian or bicycles. Simulation results and laboratory experiments show that our proposed method outperforms existing strategies. Moreover, the most impressive advantage is that the proposed strategy can plan vehicle trajectory in milliseconds, which is promising in real-world deployments. A detailed description include the coordination framework and experiment demo could be found at the supplement materials, or online at <https://youtu.be/MuhjhKfNIOg>.

Index Terms—Intelligent transportation system, autonomous vehicle, intersection coordination, motion planning.

I. INTRODUCTION

A. Background and Motivation

With the rapid development of modern industry and urbanization, more and more vehicles are entering the transportation system, which adds great pressure to the current road infrastructure. In most developed areas, there exists rather limited space to build extra flyovers and highways, to accommodate the rapidly increased number of vehicles. Meanwhile, many transportation related issues such as the safety, traffic congestion, fuel consumption, air pollution have become social problems, and received tremendous attention from various departments so far [2]–[6].

Since multiple roads merge at the road intersection, it has become one of the bottlenecks in modern transportation systems straightforwardly. According to reports in [7], most traffic congestion and accidents occur at road intersections. Traditional intersection coordination strategies include traffic

lights, roundabouts, stop signs, etc. However, 90% of traffic accidents were related to the improper behaviors of human drivers, such as the dangerous or fatigue driving, negligence of traffic coordination signals or sudden appearance obstacles [8]. Therefore, it is of vital importance to design dedicated intersection management systems to improve traffic throughput, as well as ensuring the driving safety [9].

In addition to traditional strategies, recent advances in autonomous vehicles, vehicle-to-vehicle (V2V) and vehicle to infrastructure (V2I) communications show great potential in coordination for connected autonomous vehicles (CAV), especially at non-signalized road intersections. There have been tremendous efforts on the trajectory planning of ego vehicles [10]. However, coordinators at road intersections need to handle issues from two aspects. First, CAVs are need to be carefully co-operated, to improve the traffic throughput. Second, CAVs are also need to perform ego motion planning based on environmental sensing, to avoid collisions with non-CAV-obstacles, such as pedestrians, bicycles, and other vehicles without connections.

B. Related Work

Generally, existing investigations on cooperative coordination of CAVs at road intersections could be categorized as two trends. One focused on the intersection modeling and vehicle scheduling policies, which could be termed as *Centralized* or *High-Level* planner. This High-Level planner usually has the *global information* of the entire intersection and could be physically implemented on the road side unit (RSU) or other infrastructure. One early investigation was [11], where any two CAVs were not allowed to enter the intersection simultaneously to avoid collisions. In addition to safety, this coordinator also considered other metrics such as the traffic throughput, fuel efficiency, etc. A linear maneuver model with *fixed* acceleration was considered in this piece of work, which significantly simplify the system formulation.

To further improve the throughput, Kamal *et al.* defined the cross-collision points (CCPs) at the road intersection [12]. Based on CCPs, Li *et al.* [13] proposed a cooperative critical turning point-based decision-making algorithm, which modeled the coordinator as a partially observable Markov decision processes (POMDP) problem to obtain the velocity of the critical turning points. However, the achieved velocity profiles were discontinuous, which can not be realized via practical vehicle kinematics models. Moreover, this strategy also suffered from high computational complexity.

D. Li, T. Zhang, J. Luo, T. Liang, B. Cao and Q. Zhang are with the School of Electronics and Information Engineering, Harbin Institute of Technology, Shenzhen. X. Wu is with the Communication Research Center, Harbin Institute of Technology, Harbin, P. R. China.

T. Zhang, B. Cao and Q. Zhang are also with Network Communication Research Center, Peng Cheng Laboratory, Shenzhen, P. R. China.

Email: zhangtt@hit.edu.cn

Other typical High-Level coordinators could be found in [14], [15] and references therein. The authors developed a collision set (CS) based strategy, where the coordination was formulated as a mixed integer programming (MIP) problem, and solved by introducing auxiliary variables. Since the single-CS solution was not efficient, the authors in [16]–[18] tried to extend it to a Multi-Collision Sets (MCS) model to improve the traffic capacity with a certain increase in the computational time. Moreover, authors in [18], [19] also considered the intersection *stability* when vehicles enter the intersection queue continuously, which were rarely discussed before. In all investigations above, vehicles adopted linear maneuver models, by which the coordination framework could be simplified. However, the space resources of the two dimensional intersection could not be fully exploited. In [20], the authors added the friction losses and power train into the kinematical models, to achieved more realistic solutions.

Another research trend was to adopt existing ego planners (also called as *Low-Level* planner in this paper) to the intersection coordinator, by proper modeling improvements [10], [21], [22]. There may exist two problems. First, the ego planner was mainly designed for highway driving. Therefore, when they were used in the intersection with multiple CAVs, unpredictable deadlocks, or even accidents may occur due to the greedy nature of ego planners [23]. Furthermore, most ego planners were based on a path-velocity iterative searching architecture, where was inefficient in cooperative CAV coordination. In [21], the reference paths introduced from the High-Level planner frequently made the optimization problem infeasible.

Based on the observations above, the authors in [1] firstly proposed an integrated double-level coordination framework, where the High-Level planner was used to generate the reference trajectories and corresponding feasible tunnels (FT). The Low-Level planner was similar to ego planners, and used to avoid nearby non-CAV-obstacles within the generated FT. A novel space-time resource searching (STRS) strategy was proposed at the High-Level planner, where the intersection was projected into the three-dimensional space of X, Y and T domains, and discretize it into resource blocks. After introducing the space-time resource usage as one metric in addition to traditional ones, the generated feasible tunnels could provide more efficient and balanced traffic instructions. The cost to be paid was the time consuming solutions, which may prevent its further application in real time scenarios. Aiming at this issue, Luo *et al.* proposed an efficient deep reinforcement learning (DRL) based strategy, which could generate FTs for a “bunch” of CAVs in milliseconds [24]. However, due to the vehicles grouping problem, the traffic efficiency of this method degraded in high traffic scenarios.

C. Main Contributions

Aiming at the issues on current investigations, we try to propose a low-complexity and tightly coupled bi-level coordination framework for CAVs at non-signalized road intersections. In the High-Level planner, the traffic throughput, fairness and complexity are still main considerations. Unlike

existing time exhausting investigations in [1], our method could significantly reduce the computing efforts. Furthermore, unlike the most existing *single level* coordinators, a tightly coupled Low-Level planner is proposed to handle non-CAV obstacles, which are not considered in the High-Level planner. The main contributions can be summarized as follows.

- We propose an efficient solution to indicate the feasible tunnels for each CAVs, which takes account of the various kinematics constraints and scales of CAVs. Furthermore, considering the *fairness* and the *duration of scheduling*, we give a novel benchmark of passing order priority to determine traffic sequence of vehicles.
- To ensure driving safety within the “tunnel”, we propose an effective motion plan method based on the gradient and B-spline curve. It generates the initial control points of the B-spline curve, then optimizes the control points for lower smoothness cost and avoids potential collision under the feasible tunnel constraints. Comparing to existing solutions, the tightly coupled local motion planner is more suitable to the double-level coordination framework, which could make full advantage of the result of High-Level planner.
- The simulation and laboratorial experiments show that our proposed approach can effectively improve the traffic throughput. One excellent advantage is that our High-Level planner has only millisecond-level latency, which means that the strategy can be deployed in real-world settings.

The rest of this paper is organized as follows: In Section II, we will explain the intersection model of our framework, vehicle kinematic model, the collision detection, construction of our framework and some state-of-art benchmark solutions for comparison. In section III, the modified coordination strategy based on space-time resource blocks is introduced. In section IV, a novel motion planner based on gradient is proposed, which is more suitable for the double-level framework. The simulation and laboratorial experiments results are demonstrated in Section V and Section VI, respectively.

II. PRELIMINARY

A. Intersection model

We deploy a typical road intersection which consists of R roads (for easy illustration, we set $R = 4$), as shown in Fig. 1. The width of lanes is W_L , the length of Buffer Area is L_B . The road intersection can be divided into three main sections, i.e., Waiting Area (WA), Buffer Area (BA) and Conflict Area (CA). The CA is the crucial area in our coordination framework, where potential collisions may occur.

We use $\mathcal{R} = \{1, 2, \dots, R\}$ and $\mathcal{I}_r = \{1, 2, \dots, I_r\}$ to represent the sets of roads and CAVs in road r , respectively. At signal-free intersections, the decision making center may face high dynamic scene, e.g., the unexpected obstacles, unsatisfactory communication and control systems. It is necessary to make following assumptions:

- 1) Each CAVs will send its state information (position, velocity, etc.) and intention maneuvers (i.e., go straight,

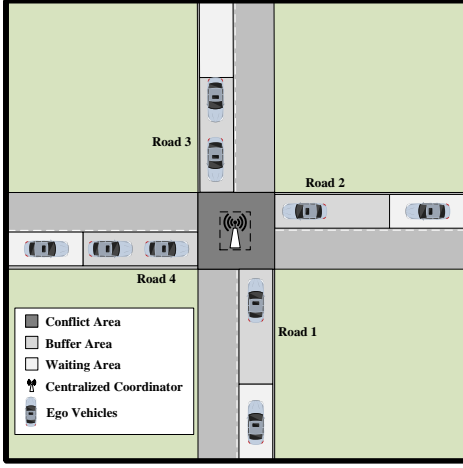


Fig. 1. System model of the intersection.

turn left and turn right) to the CC via vehicle-to-infrastructure (V2I) links, when entering the WA. After executing the coordination framework, the CC will broadcast the coordination information (i.e. the moment of entering intersection and feasible tunnels).

- 2) After received the coordination information, the CAVs should adjust their velocity in BA to enter the intersection at the timing that broadcasted by CC. Then CAVs travel along with the reference trajectory which is predefined, if there is no unexpected obstacles.
- 3) Without loss of generality, the High-Level planner will allocate the space-time resource blocks to every CAVs. Considering the unexpected obstacles, there should be some reasonable redundancy involved by the feasible tunnel to make sure the Low-Level planner has enough space to avoid collision.

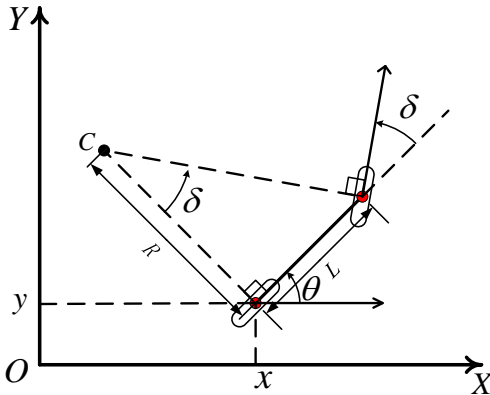


Fig. 2. The kinematic model of a front steering vehicle.

B. Vehicle Kinematic Model

In this paper, to reduce the computational complexity, we adopt the popular kinematic bicycle model [25] to describe the movement of vehicles, as shown in Fig. 2. The kinematics state of the i -th vehicle in road r can be described as

$[x_{i,r}, y_{i,r}, \theta_{i,r}, v_{i,r}]^T$, where $(x_{i,r}, y_{i,r})$, $v_{i,r}$ and $\theta_{i,r}$ are the position, velocity and heading in 2D Cartesian coordinate system, respectively. During the actual driving behavior, the control input are the longitudinal acceleration and the steering angle, donated by $a_{i,r}$ and $\delta_{i,r}$, respectively. The vehicle kinematic state update equation is shown as following:

$$\begin{bmatrix} \dot{x}_{i,r} \\ \dot{y}_{i,r} \\ \dot{\theta}_{i,r} \\ \dot{v}_{i,r} \end{bmatrix} = \begin{bmatrix} v_{i,r} \cos(\theta_{i,r}) \\ v_{i,r} \sin(\theta_{i,r}) \\ v_{i,r} \tan \delta_{i,r} / L \\ a_{i,r} \end{bmatrix}, r \in \mathcal{R}, i \in \mathcal{I}_r \quad (1)$$

where $(\bullet) := \frac{\partial}{\partial t}(\bullet)$, L_w is the distance between the front and rear wheel axles. What's more, taking into account the kinematic constraints of the vehicle, there must have:

$$\begin{aligned} a_{i,r}^{\min} &\leq a_{i,r} \leq a_{i,r}^{\max} \\ 0 &\leq v_{i,r} \leq v_{i,r}^{\max} \\ -\delta_{i,r}^{\max} &\leq \delta_{i,r} \leq \delta_{i,r}^{\max} \end{aligned} \quad (2)$$

C. Space Time Resource Blocks

The space-time resources was first used to describe the resources in the intersection by [1]. The resources in CA are described by three-dimensional coordinates in the X , Y and T domains. For the convenience of computation and reasonability, the space-time resources are divided into multiple blocks with the resolutions dx in X domain, dy in Y domain, dt in T domain. Then the resource in (x, y, z) could be described as:

$$\mathbb{B}_{j_x, j_y, j_t} = \left\{ (x, y, t) \mid \begin{aligned} (j_x - 1) \cdot dx &\leq x < j_x \cdot dx \\ (j_y - 1) \cdot dy &\leq y < j_y \cdot dy \\ (j_t - 1) \cdot dt &\leq t < j_t \cdot dt \end{aligned} \right\} \quad (3)$$

where j_x, j_y and j_t are the indexes in X, Y and T domains, respectively. One space-time can not be occupied by more than one vehicle simultaneously. Thus, when attempt to allocate the space-time resource in (j_x, j_y, j_t) , the Centralized Coordinator must the check occupancy state of the space-time resource.

The allocated area for the vehicle is represented as a collection of resource blocks, which includes not only the resource blocks occupied by the vehicle, with proper redundancy. We define the resource occupied by the i -th vehicle of road r as

$$\mathbb{A}_{i,r} = \bigcup_{(j_x, j_y, j_t) \in \mathcal{A}_{i,r}} \mathbb{B}_{j_x, j_y, j_t} \quad (4)$$

where $\mathcal{A}_{i,r}$ represents the index set of resource blocks occupied by i -th vehicle of r -th road. To keep no collisions among vehicles, we need to ensure that one resource block can only be allocated to one vehicle. That means the intersection of allocated resources between the two vehicles is empty, i.e.,

$$\mathbb{A}_{i1, r1} \cap \mathbb{A}_{i2, r2} = \emptyset \quad (5)$$

with $\forall r1, r2 \in \mathcal{R}, \forall i1 \in \mathcal{I}_{r1}$ and $\forall i2 \in \mathcal{I}_{r2}$.

D. Collision Detection

In practice, there are noises in the localization [26] and control systems,

$$\begin{cases} x_m \sim \mathcal{N}(x, \sigma_x^2) \\ y_m \sim \mathcal{N}(y, \sigma_y^2) \\ \theta_m \sim \mathcal{N}(\theta, \sigma_\theta^2) \end{cases} \quad (6)$$

$$\begin{cases} a_f \sim \mathcal{N}(a, \sigma_a^2) \\ \delta_f \sim \mathcal{N}(\delta, \sigma_\delta^2) \end{cases} \quad (7)$$

where (x, y, θ) and (x_m, y_m, θ_m) are the actual values and measured value of localization systems, respectively. (a, δ) and (a_f, δ_f) are the expected values and actual value of control systems, respectively. The CAVs always deviate from the planned trajectory. These imperfections need to be treated carefully. For the safety of vehicles, we set reasonable redundancy around the vehicle, as shown in Fig. 3. The L_{car} and W_{car} represent the length and width of vehicle, respectively. The R_{long} and R_{lat} are the longitudinal and lateral safe redundancy. The parameters of redundancy are decided by the density of obstacles and performance of control and localization system. During the coordination process and local motion planning, the redundancy region is also considered when collision detection.

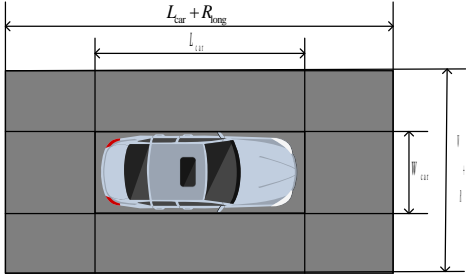


Fig. 3. The occupied region of a vehicle with safe redundancy

The space-time resource blocks occupied by other CAVs in time t could be considered as a occupancy grid map [27], as shown in Fig. 4. For a grid that has been occupied, it could not be occupied repeatedly, otherwise a collision will occur. In Low-Level planner, we assumed that the CAVs could build a OOB (Object Oriented Bounding Boxes) topological map with the equipped sensors, then transform the OOB map into the occupancy grid map.

In both High-Level and Low-Level planners, we calculate the grids that occupied by CAVs and obstacles, respectively. For collision free, there can not be any overlaps of allocated grids.

E. Structure of the Coordination Framework

The double-level coordination framework can be divided into two parts, as depicted in Fig. 5. The functions of two parts are as following.

- 1) High-Level planner (coordination strategy): After the CAVs entering the WA, the CC attempts to receive the their information about positions, velocity, intention maneuvers and the like by V2I (Vehicle to infrastructure)

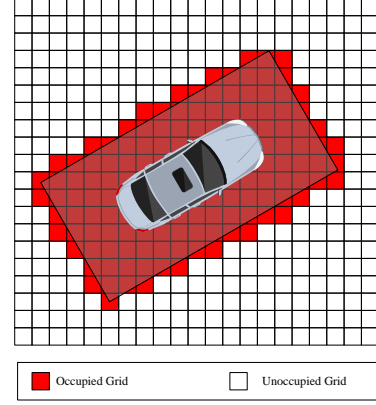


Fig. 4. The occupancy grid map of a vehicle with safe redundancy

links. According road information of the intersection, the CC generates the reference trajectories for each CAV. After calculated the traffic priority of the first CAVs in each road, the CC executes coordination strategy to get the timings of entering the intersection and feasible tunnel of the waiting CAVs.

- 2) Low-Level Planner (local motion planner): Based on the reference trajectory generated by the High-Level planner, the Low-Level planner attempts to optimize the trajectory to avoid collisions within the feasible tunnel. The practice trajectory also needs to be sufficiently smooth and feasible in terms of kinematics model. What's more, an unexceptionable controller also plays an important role in the frame, and lower control errors can reduce the probability of collisions,

F. Benchmark Solutions

In this subsection, we briefly introduce some state-of-art benchmark solutions of coordination strategy in intersection for comparison.

1) *Collision Set*: The area where exists potential collision is defined as a collision set in Collision Set (CS) strategy [18], that means one collision set can not be occupied by multiple CAVs simultaneously, the CAVs are only allowed to pass through the intersection one after the other. All though the CS strategy shows preponderance in terms of long-term stability and relative low-complexity implementation, if cannot tap the full potential of the intersection.

2) *Space-Time-Block Searching*: [1] proposed a novel and aggressive space-time resource searching (STRS) strategy. For maximum pass throughput, multiple CAVs can share the intersection simultaneously. The space-time resource is divided into many blocks which can be regarded as three-dimensional coordinates with X , Y , and T domains. Based on the reference path, CC searches the velocity profiles of CAVs in ST domains to guarantee comfort and safety. Due the transition of resources between XYT domains and ST domains, this strategy could get the optimal trajectory at the expense of high computation complexity. In comparison to CS strategy, STRS still shows a obvious throughput advantages. In addition, STRS strategy

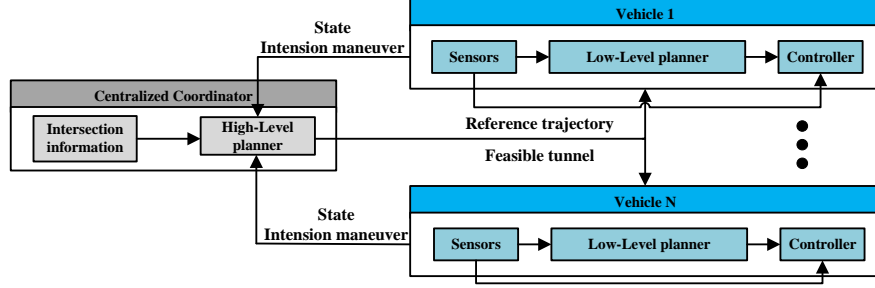


Fig. 5. The structure of coordination framework

can not operate in real-time, and the computational complexity grows exponentially.

III. HIGH-LEVEL PLANNER

The structure of the entire High-Level planner is shown in Fig. 6. Firstly, we generate reference trajectories of different CAVs according to their kinematic constraints by Reference Trajectory Generator. We can obtain the reasonable timing of CAVs to enter the intersection by the core module of our proposed, then the CC determines the current round passage CAV by comparing the priority of CAVs, and allocates its feasible tunnel to complete the current round of coordination. As the result of the High-Level planner is the timing of the CAV to enter the Conflict Area, the trajectory between the Waiting Area and the Conflict Area needs to be calculated finally. We'll introduce each of the modules mentioned above.

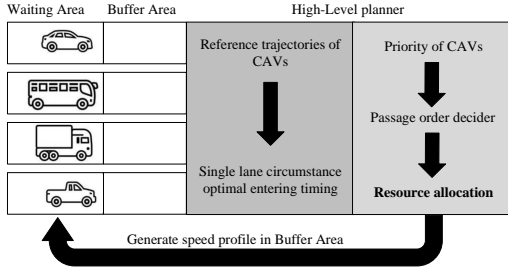


Fig. 6. The structure of High-Level planner

A. Reference Trajectory Generator

The simplified line & circle path [28] is one popular option. However, it is too ideal to be realized in the kinematic bicycle model due to the discontinuous second order derivative. In the three-dimensional Cartesian coordinates system XYT, the trajectory can be decoupled as Path and Speed Profile [29]. Usually, the trajectory can be expressed as

$$\begin{cases} \text{Path: } \begin{cases} x = f(s) \\ y = g(s) \end{cases} \\ \text{Speed Profile: } s = s(t) \end{cases} \quad (8)$$

where s is the arc length along with the path, u is decided by velocity and acceleration of vehicle.

In order to make the path smooth and subject to the kinematics constraints, the problem can be built as a constrained optimization problem, one key constraint is the continuity of trajectories [22].

$$\begin{aligned} f(0) &= x_0, g(0) = y_0 \\ f(s_t) &= x_{s_t}, g(s_t) = y_{s_t} \end{aligned} \quad (9)$$

where (x_0, y_0) and (x_{s_t}, y_{s_t}) are the start and end position of standard line & circle path, respectively. s_t is the total length of standard path.

In order to make the reference trajectory more consistent with traffic rules and human driving habits, the distance limitation between the actual path and the standard line & circle path is also a necessary constraint.

$$\begin{aligned} |f(s_j) - x_j| &\leq d_b \\ |g(s_j) - y_j| &\leq d_b \end{aligned}, \forall j \in \{1, 2, \dots, N_s\} \quad (10)$$

where (x_j, y_j) are the equally spaced sample points on standard line & circle path. N_s is the number of sample points, which is decided by Δs . d_b is the distance limitation between reference and standard line & circle paths.

Therefore, the optimization problem can be expressed as

$$\begin{aligned} \mathcal{P}_1 : \min. & \sum_{i=2}^4 \omega_i^{\text{ref}} \int (f^{(i)}(s))^2 + (g^{(i)}(s))^2 ds \\ \text{s.t.} & (9), (10) \end{aligned} \quad (11)$$

where $\bullet^{(i)}(s)$ means the i -th order derivative of $\bullet(s)$.

Generally, the quintic polynomial is a good way to express the trajectory, then \mathcal{P}_1 can be formulated as a typical quadratic programming (QP) problem [30], and solved by off-the-shelf solvers rapidly.

Since the length of entire standard line & circle path s_t will be changed after planning, we propose a method to generate speed profiles rapidly for the higher fuel efficiency [14] and comfort. Ideally, we want the vehicle to cross the intersection with a speed close to the reference speed v_{ref} without any accelerations. After solving the reference path, we can obtain the length of the reference path s_n , thus the speed profile can be expressed as

$$s(t) = \frac{s_t}{s_n} v_{\text{ref}} t \quad (12)$$

B. Trajectory in Buffer Area

Usually, the CAVs in the Waiting Area can not accelerate to the reference speed instantaneously, due to vehicle kinematics limitations. It is necessary to set a Buffer Area for the vehicle to adjust their speed.

Considering the size of the CAV and redundancy, we use part of the Buffer Area with a length of L_A for adjusting the speed. Obviously the path in that area is a straight line. We use the quintic polynomial to represent the speed profile, and to ensure continuity, constrain the position, velocity and acceleration at the endpoints. Typically, the CAVs are initially stationary in the Buffer Area, the mathematical expressions of the six constraints are as follows,

$$\begin{aligned} s_B(0) = 0, \quad s_B^{(1)}(0) = 0, \quad s_B^{(2)}(0) = 0 \\ s_B(t_a) = L_A, \quad s_B^{(1)}(t_a) = s^{(1)}(0), \quad s_B^{(2)}(t_a) = s^{(2)}(0) \end{aligned} \quad (13)$$

where $s_B(t)$ represents the speed profile in Buffer Area. For non-stationary CAVs, this method can respond flexibly by changing the constraints.

Since the quintic polynomial has six unknowns and we have six constraints, it is straightforward to solve the coefficients of quintic polynomial in closed forms. For a larger Waiting Area, we can also generate velocity profile in a similar way to the Reference Path Generator, which we will not discuss here.

C. Problem Formulation

The High-Level planner of STRS strategy can not solve in real-time, because of the high computation complexity. In order to apply the double-level framework based on space-time resource block to multi-roads intersection, we improved the model to overcome the high computation complexity and propose a new High-Level planner to achieve feasible tunnel allocation for higher efficiency in traffic utilization.

First, the CC should calculate the reference trajectory for each vehicle. Specially, the potential collision exists in the Conflict Area, so we only consider the reference trajectory between the vehicle and redundancy entering the Conflict Area and leaving the Conflict Area. Then, the reference trajectory of i -th vehicle in road r can be represented as following,

$$\text{Trajectory: } \begin{cases} x_{i,r}(t) = f_{r_i,r_i,m}(t - t_{i,r}^e) \\ y_{i,r}(t) = g_{r_i,r_i,m}(t - t_{i,r}^e) \\ \theta_{i,r}(t) = \arctan \frac{f'_{r_i,r_i,m}(t - t_{i,r}^e)}{g'_{r_i,r_i,m}(t - t_{i,r}^e)} \end{cases}, \quad (14)$$

$$0 \leq t - t_e \leq t_{r_i,r_i,m}$$

where r_f and r_t are the road which the vehicle come from and intend to reach, respectively. Specifically, m is the maneuver (turn left, go straight, turn right) of the vehicle, that means road r_t must be one of the feasible roads, which vehicle came from r_f road and maneuvered as m could reach. $t_{i,r}^e$ and $t_{r_i,r_i,m}$ are the moments of entering the Conflict Area and the duration of the specified reference trajectory, respectively. We can calculate the index set $\mathcal{C}_{r_i,r_i,m}^t$ of resource blocks occupied by vehicle at time t state directly.

Generally, the index set of occupied resource block of each trajectory starting at time t^e are represented as

$$\mathcal{D}_{r_i,r_i,m}^{t^e} = \left\{ (j_x, j_y, j_t + \left\lfloor \frac{t^e}{dt} \right\rfloor) \mid \bigcup_{0 < t < t_{r_i,r_i,m}} \mathcal{C}_{r_i,r_i,m}^t \right\} \quad (15)$$

where $\lfloor \bullet \rfloor$ means the round down of \bullet . $\mathcal{C}_{r_i,r_i,m}^t$ means the index set of resource blocks which are occupied vehicle with (r_f, r_t, m) state at time t . Because the starting time of reference trajectory provided by Reference Trajectory Generator is 0, the time index of reference trajectory index set must be added with a time offset $\lfloor \frac{t^e}{dt} \rfloor$.

D. Single Lane Circumstance

When there's only one road need to be coordinated, CAVs could only enter the intersection one by one. Thus, we should indicate the timing of entering the intersection for each CAVs.

At k -th round, the index set of space-time resource blocks occupied in previous $1 \sim k-1$ rounds can be expressed as $\mathcal{A}_{\text{pre}}^k$. Particularly, $\mathcal{A}_{\text{pre}}^1 = \emptyset$ in the first round. For potential collisions avoidance, we need to guarantee that the same resource block cannot be occupied repeatedly, i.e.,

$$\mathcal{D}_{r_i,r_i,m}^t \cap \mathcal{A}_{\text{pre}}^k = \emptyset \quad (16)$$

At k -th round, the resource that allocated to the i -th vehicle in r -th road can be represented by $\mathcal{A}_{i,r}^k = \mathcal{D}_{r_i,r_i,m}^t$. After k -th round, \mathcal{A}_{pre} should be updated.

$$\mathcal{A}_{\text{pre}}^{k+1} = \mathcal{A}_{i,r}^k \cup \mathcal{A}_{\text{pre}}^k \quad (17)$$

Thus, the resource allocation problem can be described as a typical linear programming problem:

$$\begin{aligned} \mathcal{P}_2 : \min. \quad & \max. \{j_t \mid j_t \in \mathcal{A}_{\text{final}}\} \\ \text{s.t.} \quad & (5) \end{aligned} \quad (18)$$

where $\mathcal{A}_{\text{final}}$ represents the index set of resource blocks occupied during the whole scheduling process.

But unusually, this optimization problem is an NP-Hard problem, and solved by conventional solution methods would consume a lot of computational resources, so we choose to decompose this optimization problem into sequence optimization problem to solve.

E. Priority of CAVs

When there are CAVs in multiple roads to be coordinated, the coordination framework needs to decide the CAVs' priority. Based on the resource blocks allocated to vehicle, the priority term of scheduling duration P_d could be defined as

$$P_d = w_d \cdot \max \{j_t \mid j_t \in (\mathcal{A}_{i,r}^k \cup \mathcal{A}_{\text{pre}}^k)\} \cdot dt \quad (19)$$

The general intersection coordination strategy all aim to maximize throughput, that can lead to unfair situations where the first CAV at some roads cannot be scheduled for a long time. [1] also ensures the fairness of the passage by introducing resource occupancy rate term into the performance criteria of the coordination. Nevertheless, vehicles going straight tend to increase resource occupancy rate more than turning left

in most cases. In practice, the reasonableness of this item is debatable. An effective approach is to add waiting time term to the performance criteria of the coordination for fairness of passage.

$$P_w = \omega_w \cdot \sum_{n=1}^i \frac{t_{\text{waiting}}^n}{n} \quad (20)$$

where t_{waiting}^n indicates the waiting time at n -th in road queue.

For queue stability [31], according to Lyapunov theorem, we should ensure the following equation holds,

$$\lim_{T \rightarrow \infty} \sup \frac{1}{T} \sum_{t=1}^T E[l_r(t)] < \infty, r \in R \quad (21)$$

where $l_r(t)$ is the length of r -th road at t .

Thus the performance criteria about queue stability can be defined as:

$$P_{\text{sta}} = \omega_{\text{sta}} \cdot l_r(t) a_r^{\text{av}} \quad (22)$$

where a_r^{av} represents the arrive rate of r -th road.

In every round, we could select the optimal vehicle v in all road to pass base on priority of vehicle function, i.e.,

$$v = \arg \min \{P_d + P_w - P_{\text{sta}}\} \quad (23)$$

Specially, v must be the first vehicle in all road queue in this round.

The algorithm flow of the entire High-Level planner is shown in Algorithm 1.

Algorithm 1 High-Level Planner

- 1: Initialization. Set initial CAVs $\forall r \in \mathcal{R}, \forall i \in \mathcal{I}_r$, set $k = 1$ and $\mathcal{A}_{\text{pre}}^1 = \emptyset$.
 - 2: Get the information of intersection and vehicle, generation standard reference trajectories.
 - 3: **repeat**
 - 4: **for** each $r \in R$ **do**
 - 5: Calculate the priority of first vehicle in road according 23.
 - 6: **end for**
 - 7: Select the optimal vehicle v .
 - 8: $j_t = 0$.
 - 9: **repeat**
 - 10: $j_t = j_t + 1$.
 - 11: **until** $\mathcal{D}_{r_t, r_t, m}^{j_t} \cap \mathcal{A}_{\text{pre}}^k = \emptyset$
 - 12: Allocate resource for vehicle v , i.e., $\mathcal{A}_{i, r}^k = \mathcal{D}_{r_t, r_t, m}^{j_t}$
 - 13: Update allocated resource, $\mathcal{A}_{\text{pre}}^{k+1} = \mathcal{A}_{i, r}^k \cup \mathcal{A}_{\text{pre}}^k$
 - 14: $k = k + 1$.
 - 15: **until** The co-scheduling process is complete.
-

IV. LOW-LEVEL PLANNER

For CAVs, there exist various random obstacles, such as pedestrians, bicycles, etc. They usually cannot be accurately tracked or predicted by road infrastructures, so such obstacles cannot be considered in the High-Level planner. In addition, due to imperfect control and localization operations, CAVs may move out of their feasible tunnel and collide with other

CAVs. The CAVs need to characterize obstacles and the environment to generate the actual trajectory based on the reference trajectory and feasible tunnel provided by High-Level planner.

The reference trajectory provided by High-Level Planner is optimal, since Reference Trajectory Generator problem was modeled as a quadratic programming problem. The optimality and feasibility of the reference trajectory will be destroyed due to the consideration of obstacles. The existing approach is to discard the original reference trajectory and recalculate the path and speed profile in the convex feasible tunnel. Obviously, recalculating the trajectory with DP+QP strategy is extremely time challenging.

Theoretically, the coordination efficiency of the High-Level Planner is closely related to the redundancy size, and the DP+QP method generally uses a circular collision detection model, which leads to large and inefficient redundancy, so a fast and efficient low-level planner is necessary to be proposed.

A. Problem Formulation

Inspired by [32], we propose a gradient optimization-based trajectory generation scheme. In addition to the reference trajectory, we further consider four more factors: smoothness, kinematic feasibility, energy efficiency and collision avoidance, which can effectively avoid the time consuming trajectory re-calculation. The trajectory is represented by a p_d -th order uniform B-Spline curve, and can be optimized by the control points of the B-Spline curve \mathbf{Q} by gradient of the cost function. The original control points of B-Spline curve can be calculated by reference trajectories.

In general, the maneuver smoothness can be characterized via the acceleration, jerk and snap [30], specifically, the snap can be ignored when $p_d \leq 3$. The kinematics feasibility cost is represented by the limitation of lateral acceleration. In terms of fuel efficiency, the optimal velocity profile is a constant v_{ref} [14]. Intuitively, we try to minimize the longitudinal acceleration, to approach the expected constant velocity. Thus, the smoothing, kinematics feasibility and energy efficiency terms of cost function can be expressed as following:

$$C_s + C_k + C_e = \sum_{i=2}^3 \omega_i \int \left\| \mathbf{h}^{(i)}(t) \right\|_2^2 dt \quad (24)$$

where $\mathbf{h}(t) = [f(t) \ g(t)]$.

The B-Spline curve is convex, which indicates that a span B-Spline curve can be controlled by $p_d + 1$ successive control points. Another property is that the k -th order derivative of a B-Spline curve is also a B-Spline curve with $p_{d,k} = p_d - k$. In our study, $p_d = 3$, the 3-th order derivative of a single span B-Spline curve is a constant, the snap term can be ignored in cost function [33].

For uniform B-Spline curve with N_c control points, the number of knots is $p_d + N_c + 1$, the knots vector can be represented by $\mathbf{t}_k = [t_0, t_1, \dots, t_{p_d+N_c}]^T$ with constant interval Δt . The velocity \mathbf{V}_i , acceleration \mathbf{A}_i and jerk \mathbf{J}_i can be obtained by

$$\mathbf{V}_i = \frac{\mathbf{Q}_{i+1} - \mathbf{Q}_i}{\Delta t}, \mathbf{A}_i = \frac{\mathbf{V}_{i+1} - \mathbf{V}_i}{\Delta t}, \mathbf{J}_i = \frac{\mathbf{A}_{i+1} - \mathbf{A}_i}{\Delta t}, \quad (25)$$

Thus, the cost function can be rewritten as

$$C_s + C_k + C_e = \omega_{\text{acc}} \sum_{i=0}^{N_c-2} \|\mathbf{A}_i\|_2^2 + \omega_{\text{jerk}} \sum_{i=0}^{N_c-3} \|\mathbf{J}_i\|_2^2 \quad (26)$$

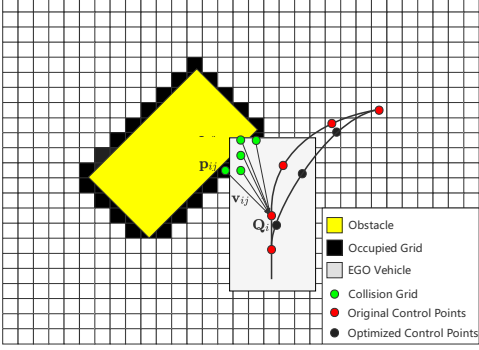


Fig. 7. Generation of collision term in cost function

B. Collision Avoidance

The most difficult part of the Low-Level planner is the cost function with obstacle avoidance. In [32], it is only applicable to objects with round or square outlines. The state of dynamic obstacles can be observed through proper prediction algorithms [34]. In a typical turning scenario, as shown in Fig. 7, when $t = t_{i+2}$, $t_{i+2} \in \mathbf{t}_k$ $0 \leq i < N_c$, \mathbf{Q}_i has the highest weight for the position of trajectory. We check whether there are potential collisions at $t = t_{i+2}$. With the predictor we can get the position and state of the obstacles and the grid occupied by the obstacles can be obtained. Record the j -th potential collision grids nearby \mathbf{Q}_i as \mathbf{p}_{ij} , then the gradient generation vector can be calculated by

$$\mathbf{v}_{ij} = \mathbf{Q}_i - \mathbf{p}_{ij}. \quad (27)$$

Theoretically, the closer the collision point, the greater the cost. A reasonable piecewise polynomial loss function is necessary, which is twice continuously differentiable. First, if the collision points are within a circle with the vehicle center as the center of circle and the diagonal of vehicle as the diameter, it will apply a higher penalty to the control points. Considering the error of control model and the grid size, we set an additional redundancy to keep collision-free, which apply a lower penalty. Finally, the piecewise polynomial function [32] of collision avoidance can be represented by

$$C_c(i, j) = \begin{cases} 0 & (d_{ij} < 0) \\ d_{ij}^3 & (0 \leq d_{ij} < d_r) \\ 3s_f d_{i,j}^2 - 3s_f^2 d_{i,j} + s_f^3 & (d_r \leq d_{ij}) \end{cases} \quad (28)$$

where $d_{ij} = d_r + d_f - \|\mathbf{v}_{ij}\|_2$, d_r and d_f are the additional redundancy distance and the diagonal of CAV, respectively. $C_c(i, j)$ is the collision cost value of \mathbf{Q}_i caused by collision grid \mathbf{p}_{ij} . The total collision cost of \mathbf{Q}_i can be evaluated independently, i.e., $C_c(\mathbf{Q}_i) = \sum_{j=0}^{N_i-1} C_c(i, j)$, N_i is the

number of collision grid of \mathbf{Q}_i . Then the collision cost of entire trajectory can be evaluated by all control points.

$$C_c = \omega_c \sum_{i=0}^{N_c-1} C_c(\mathbf{Q}_i) \quad (29)$$

For the gradient of collision term, it can be evaluated by the derivative of C_c with respect of \mathbf{Q}_i directly.

$$\frac{\partial C_c}{\partial \mathbf{Q}_i} = \sum_{j=0}^{N_i-1} \frac{\mathbf{v}_{ij}}{\|\mathbf{v}_{ij}\|_2} \begin{cases} 0 & (d_{ij} < 0) \\ -3d_{ij}^2 & (0 \leq d_{ij} < d_r) \\ -6s_f d_{i,j} + 3s_f^2 & (d_r \leq d_{ij}) \end{cases} \quad (30)$$

C. Trajectory Optimization

The trajectory optimization problem considering collision avoidance can be modeled as an unconstrained optimization problem as (31), which uses some tricks to achieve approximate hard constraints.

$$\mathcal{P}_2 : \min_{\mathbf{Q}} C_s + C_k + C_e + C_c \quad (31)$$

We generate the control points of the B-Spline curve with the sampling points and states of the start and end points of the reference trajectory. In order to ensure that the higher order derivative of the start and end points are continuous, the first three and last three control points cannot be optimized, which means that the number of control points must be greater and equal than 7. Since the objective function is higher than quadratic and quadratic terms dominate, the Hessian matrix can be used to accelerate the optimization process. In [32], L-BFGS method [35] has a good performance in unconstrained optimization, thus, we optimize the control points with L-BFGS method.

We set virtual obstacles on the boundary of the feasible tunnel to ensure that CAVs can not move out. After optimization, collision may still exist or the trajectory is not smooth enough, we can optimize again by increasing the weight of the corresponding term to make the trajectory meet the constraints, but in most cases, once is enough.

V. SIMULATION RESULTS

In this section, we performed simulations in a typical four-lane road intersection scenario as shown in Fig. 1, to demonstrate the performance of our proposed method. we compare it with the existing solutions in Section II-F. We consider only the space-time resources within the intersection Conflict Area. The reference trajectory of the vehicle is given by Section III-A and III-B.

A. High-level planner

Fig. 8 shows the reference trajectory provided by the Reference Trajectory Generator, which avoids the flaw of line & circle curve paths and improves smoothness and feasibility. Theoretically, the Reference Trajectory Generator is scalable in multi-lane road intersections.

TABLE I
CALIBRATION OF MAIN PARAMETERS

Parameters	Value	Parameters	Value
W_L, L_B	4m, 8m	d_b	1.0m
$\omega_2^{\text{ref}}, \omega_3^{\text{ref}}, \omega_4^{\text{ref}}$	1, 1, 1	v_{ref}	8m/s
dx, dy	0.2m	dt	0.2s
$L_{\text{car}}, W_{\text{car}}$	4m, 2m	a_r^{av}	0.8
$R_{\text{long}}, R_{\text{lat}}$	0.5m, 0.5m	$\omega_{\text{acc}}, \omega_{\text{jerk}}$	5, 1
$\omega_d, \omega_w, \omega_{\text{sta}}$	$1, 5 * 10^{-1}, 1.0$	ω_c	0.1
d_r, d_f	0.5m, 2.5m		

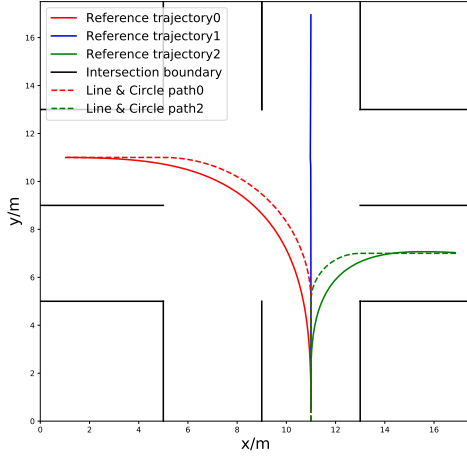


Fig. 8. The reference path and line & circle path

1) *Space-Time Resource Allocation*: For four left-turning CAVs from different roads, theoretically, it is a reasonable solution that CAVs enter the intersection in sequence. The same strategy is given in our experiments. Fig. 9 shows the reference trajectories and resource allocations of the CAVs in this scenario, we only set $dt = 0.05\text{s}$ in particular simulation for better illustration of space-time resource blocks.

In this result, the resource blocks of different CAVs touch on the t-axis, which indicating that the CAVs pass through the road intersection without collision. This essentially shows that single vehicle finds the optimal solution, i.e. the fastest solution to get through the road intersection, subject to the order of passage provided by the High-Level Planner.

2) *Speed Profile Analysis*: In a typical four left-turn CAVs scenario, Fig. 10 represents the output of our proposed method compared with CS and STRS in ST coordinate system of Frenet Frame [29], respectively. In Fig. 10(a), since the solution of CS strategy is that the road intersection can be occupied by only one vehicle at the same time, the latter vehicle must enter the intersection after the former one has left, this strategy leads to a less efficient intersection passage.

In Fig. 10(b), unlike the CS and our proposed approach, the STRS strategy adjusts the speed profile by DP+QP to find the optimal solution. Since the goal of the STRS strategy is to find the optimal solution of comfort and fuel efficiency without collision for each vehicle, which is often not optimal for pass

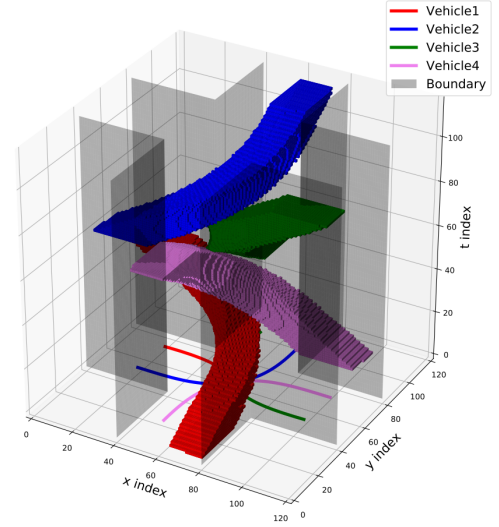


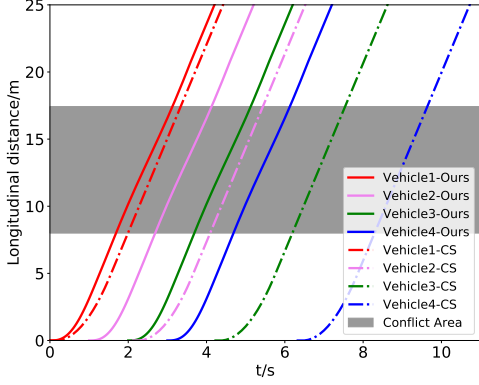
Fig. 9. The reference trajectories and resource allocation for four left-turning CAVs from different lanes

throughput.

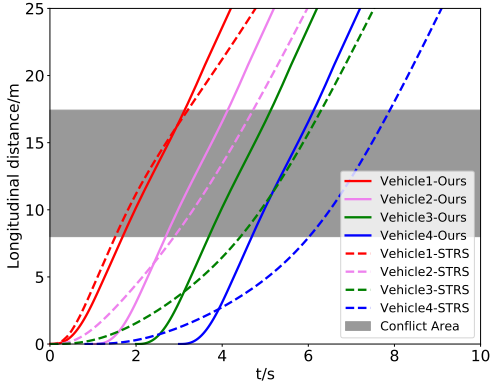
The key issue of our proposed strategy is to ensure that the space-time resource blocks do not overlap, to guarantee safety. While the trajectory comfort could be guaranteed by the reference trajectory. Therefore, combining the results of the three strategies above, our proposed method improves the traffic throughput compared to the CS strategy, but the comfort level is not as high as STRS.

3) *Waiting Time Term*: We set up an extreme simulation scenario where there are three CAVs going straight on Road 1 and Road 2 respectively, and three CAVs turning left on Road 2 and Road 4 respectively. Fig. 11(a) shows the resource allocation results without considering the waiting time term, where the resources allocation for CAVs from different roads are distinguished by different colors. Because CAVs going straight have shorter distances and can move out the intersection earlier, the High-Level Planner prefer to raise the priority of CAVs going straight, which would lead to unfairness. In Fig. 11(b), with the introduction of the waiting time term to priority, the scheduler will avoid the situation that long waiting time of the first vehicle in road queue and ensure the fairness of CAVs with different maneuvers in different roads.

4) *Total Passing Time*: Due to the different objectives of the High-Level coordination method, it mainly faces the contradiction between comfort and traffic efficiency. Therefore, the actual performance of the algorithm cannot be explained by directly comparing the total passing time of same traffic flow. We generate two kinds of traffic flows to compare the ability of different methods to tap the potential of the road intersection in the face of different traffic flows. Traffic flow 1 consists of 50% left-turning CAVs, right-turning CAVs and straight-going CAVs accounted for 25% each. Traffic flow 2 consists of 50% straight-going CAVs, 25% right-turning CAVs and 25% left-turning CAVs. Fig. 12 shows the total passing time of CS, STRS, and our proposed approach versus the number of vehicles when facing different traffic flows.



(a) Comparison of our proposed method and CS strategy in ST coordinate system

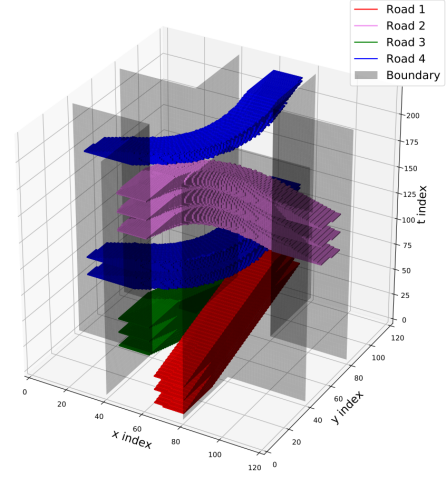


(b) Comparison of our proposed method and STRS strategy in ST coordinate system

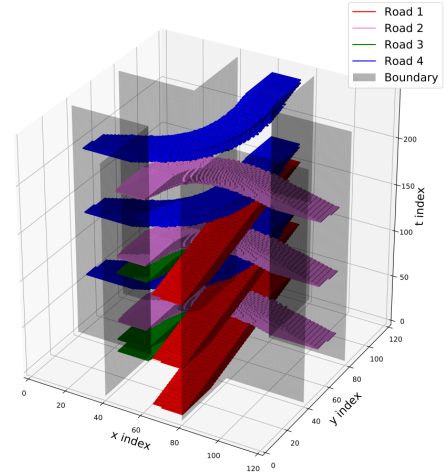
Fig. 10. Comparison of different methods in ST coordinate system

Just like the conclusion of [V-A2](#), due to the waste of resources, CS strategy can not make the most of the resources at the crossroads and has the lowest traffic efficiency of the road intersection. Because in the face of different traffic flows, the two total passing time did not widen the gap. The STRS strategy try to find the optimal solution of comfort and fuel efficiency, which means that the total passing time of STRS strategy is not always the optimal. However, this method can greatly realize the potential of intersections in the face of traffic flow with more straight traffic. Similar to STRS, our proposed approach can also ensure the efficiency of intersections in the face of different traffic flows. which sacrifices some comfort and achieves an increase in intersection throughput. Nonetheless, a possible corollary is that modifications to the optimization objective in STRS strategy can theoretically lead to an optimal solution for the passage efficiency, since the STRS strategy searches all speed profiles at a certain resolution iteratively.

5) *Computation Time*: In Fig. 13, we can observe an crucial phenomenon that the computation time performance of our proposed strategy significantly outperforms other strategies. Since the CS strategy introduces an auxiliary variable to



(a) Resource allocation without waiting time term



(b) Resource allocation with waiting time term

Fig. 11. Illustration of resource allocation in the extreme scenarios

guarantee the presence that only one vehicle within the intersection, this implies that the optimization is a mixed-integer programming. For the STRS strategy, the main computation time is consumed in two processes, one is the projection of the resource blocks occupied by other CAVs onto the Frenét Frame with the reference path of current vehicle as the reference line, and the other one is that searching iteratively for all possible speed profiles by DP. As the number of CAVs increases, the number of resource blocks to be projected grows, so it is not a wise choice to use the STRS strategy in the actual implementation even in a platform with very high arithmetic.

Since the trajectory is predetermined and the process of calculating the velocity profile one by one is omitted, which result in the optimization model becomes a linear programming model, which means that we can solve it with an unexceptionable computational performance on the premise of ensuring comfort.

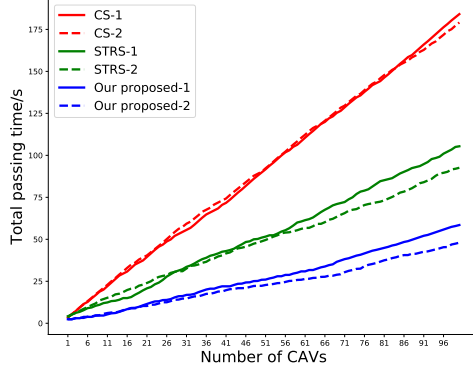


Fig. 12. The total passing time of the three strategies

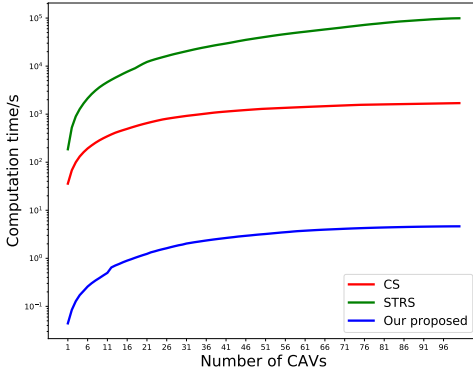


Fig. 13. The computation time of the three strategies

B. Low-Level Planner

1) *Trajectory Analysis*: Fig. 14 shows a simulation results comparison between our proposed and the DP+QP [22] strategy, the gray area is an obstacle projected into the Frenét Frame, the solid line is the result of DP+QP strategy, and the dashed line is the simulation result our proposed method. The simulation parameters are listed in Table. II. both of them generate a reasonable trajectory. Nevertheless, analyzing the curvature of the trajectory we can find that the curvature of the trajectory generated by the Low-Level planner of DP+QP is not smooth enough. The front wheels will shake violently due to the uneven curvature. Notably, greater curvature means higher potential to exceed the limitations of kinematic models [36].

2) *Computation Time*: During the simulation, we found that potential collisions due to suboptimal control and positioning systems can be avoided simply by using the path planner.

TABLE II
CALIBRATION OF MAIN PARAMETERS

Parameters	Value	Parameters	Value
Δt	1.0s	d_r	2.5m
L_{car}, W_{car}	4.72m, 1.88m	d_f	0.94m
$\omega_{acc}, \omega_{jerk}, \omega^c$	0.1, 5.0, 1.0	R_{long}, R_{lat}	0.5m, 0.5m

Normally these two modules do not cause aggressive errors. Therefore, in this part of the simulation, we only compare the simulation time of the Path Planners. However, we still list the computation time of the DP+QP strategy Low-Level Speed Profile Planner. In practical deployments, Low-Level Planners are accelerated by parallel computing, which often leads to unfair computation resource allocation during the simulation phase, so we simply use single-threaded in order to reach a uniform conclusion. In Table. III, an important conclusion is demonstrated, i.e., the strategy of DP+QP consumes a lot of time to search out the optimal path by DP, even though the optimal path is not much better than the suboptimal path frequently. Our proposed method consumes less time to optimize the existing reference path. Shorter computing times mean CAVs have longer time to respond to emergencies.

TABLE III
THE COMPUTATION TIME

	Path/ms	Speed Profile/ms
Our proposed	99.150299	
DP+QP [1]	412.091	1563.254

VI. LABORATORY EXPERIMENTS

Finally, in order to verify the feasibility and robustness of our proposed double-level coordination strategy, we used four autonomous mobile robots with robot operating systems (ROS) [37] to complete the laboratory experiments. We used the desktop computer to run the High-Level planner, distributed the results of the High-Level planner to the mobile robot through ROS network communication, and the Low-Level planner was completed with the mobile robot onboard computers. In order to conform to the reality, we mainly adjusted the experimental parameters: $dx = dy = 0.05m$, $\Delta t = 0.1s$, $L_{car} = 0.44m$, $W_{car} = 0.34m$.

Fig. 16 shows the mobile robot we used, which is equipped with Intel T265 tracking camera and D455 depth camera. In this experiment, we only used T265 for online localization, and perceptual results were generated offline. In addition, we use the Intel NUC microcomputer as the onboard computer, and the sufficient computing resources enable the platform to ensure real-time performance.

A. High-Level planner experiment I

Fig. 17 shows a typical laboratory road intersection scenario. In this experiment, four mobile robots all adopt a left turn strategy. We use large safety redundancy and fast reference speed, i.e., $R_{long} = R_{lat} = 0.4m$, $v_{ref} = 0.4m/s$. In this experiment, due to the large safety redundancy, CAVs in the diagonal roads cannot enter the intersection simultaneously, thus, the CAVs need to enter the intersection one by one. We plotted the reference path of CAV1 with red curve to show the error of the control system. With proper security redundancy, our proposed can realize the throughput potential of the intersection without collision.

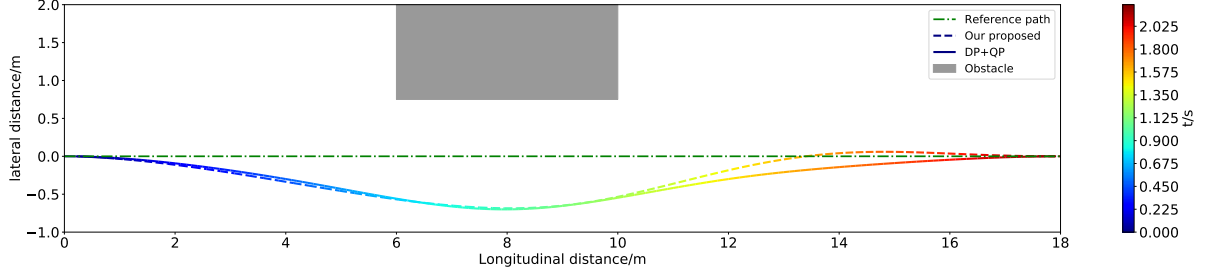


Fig. 14. Comparison of simulation results between DP+QP [22] and our proposed solution in Frenét Frame

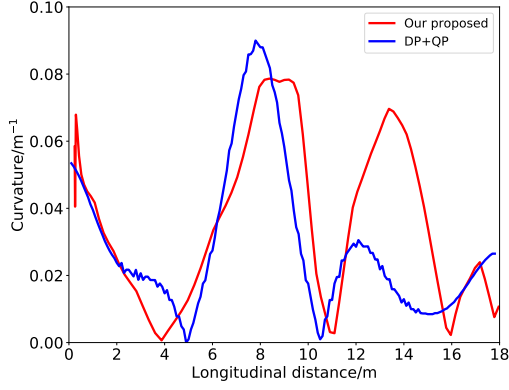


Fig. 15. Curvature (m⁻¹) versus Longitudinal distance (m).

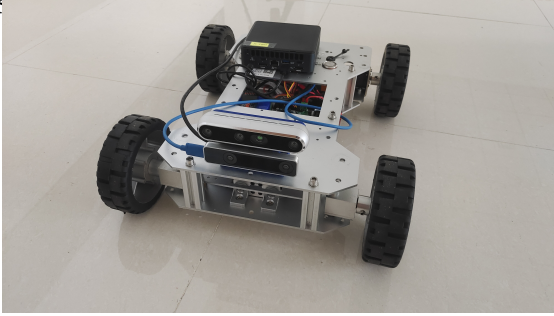


Fig. 16. Autonomous mobile robots used in experiments

B. High-Level planner experiment II

In Fig. 18, We reduce security redundancy, i.e., $R_{\text{long}} = R_{\text{lat}} = 0.1\text{m}$. We plotted the reference paths of CAV1 and CAV3 with red curves, their reference trajectories don't conflict, thus, the CAVs from the diagonal roads can enter the road intersection simultaneously.

C. Double-level coordination strategy experiment

With unexpected obstacles in the intersection or a large control error, coordination strategy requires the intervention of the Low-Level planner. In this laboratory experiment, we adopt relatively lower reference speed ($v_{\text{ref}} = 0.2\text{m/s}$) and same redundancy with High-Level planner experiment I. A static obstacle is arranged in the intersection, which is marked by red box. As a result of this obstacle, the reference trajectory of the CAV2 is exposed to potential collision. After spotting the obstacle, CAV2 generates the collision free trajectory base

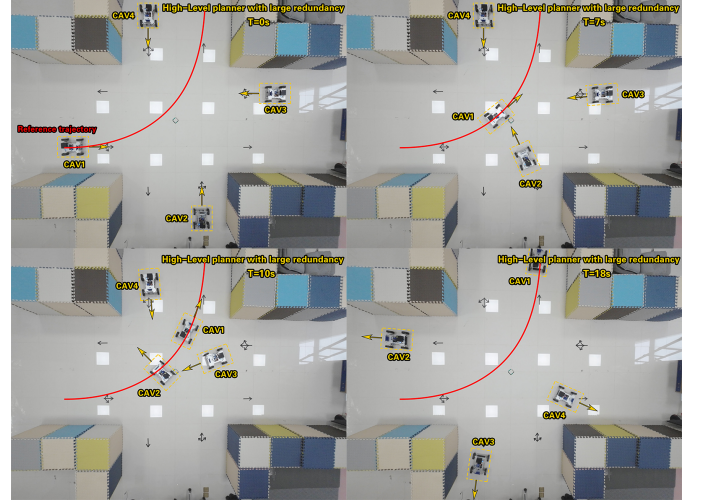


Fig. 17. High-Level planner laboratory experiments with large redundancy

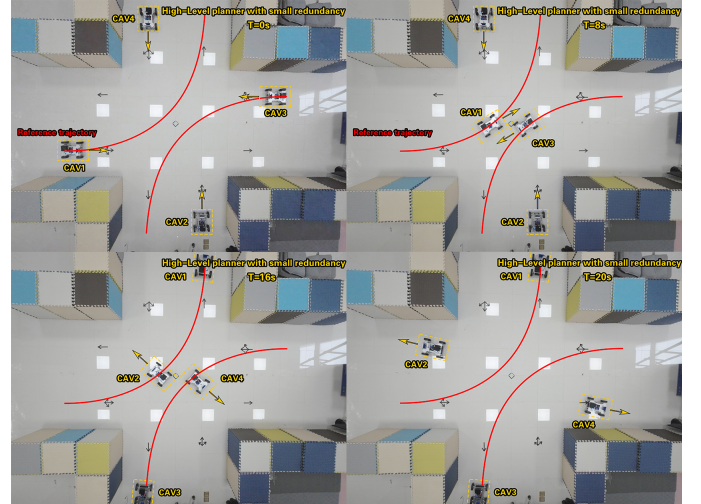


Fig. 18. High-Level planner laboratory experiments with small redundancy

on the result of High-Level planner by Low-Level planner. Fig. 19 shows the results of the experiment.

VII. CONCLUSION

In this paper, We try to give a tightly coupled two level coordination framework for CAVs at non-signalized road intersections. Aiming at the computational complexity at the



Fig. 19. Double-level coordination strategy experiment with unexpected obstacle in intersection

High-Level planner, we decouple the original problem into sequential optimization ones, to generate the available space and time resource blocks, namely feasible tunnels, for each vehicle. Furthermore, a Low-Level planner is also given under the constraints from FTs, to avoid potential collisions with unexpected non-CAV obstacles. We provide numerical results via simulations and laboratory experiments, which could achieve coordination within millisecond level. Although the uncertainties during coordination could be accommodated by the redundancy design of FTs, it is still prone to severe errors from sensing, control and communications. The robustness issue of this two-level coordinator will be discussed in our future work.

REFERENCES

- [1] Y. Zhang, R. Hao, T. Zhang, X. Chang, Z. Xie, and Q. Zhang, "A trajectory optimization-based intersection coordination framework for cooperative autonomous vehicles," *IEEE Transactions on Intelligent Transportation Systems*, vol. 23, no. 9, pp. 14 674–14 688, 2022.
- [2] M. Alsabaan, W. Alasmay, A. Albasir, and K. Naik, "Vehicular networks for a greener environment: A survey," *IEEE Communications Surveys & Tutorials*, vol. 15, no. 3, pp. 1372–1388, 2013.
- [3] S. Dornbush and A. Joshi, "Streetsmart traffic: Discovering and disseminating automobile congestion using vanet's," in *2007 IEEE 65th Vehicular Technology Conference - VTC2007-Spring*, 2007, pp. 11–15.
- [4] P. G. Shinde and M. M. Dongre, "Traffic congestion detection with complex event processing in vanet," in *2017 Fourteenth International Conference on Wireless and Optical Communications Networks (WOCN)*, 2017, pp. 1–5.
- [5] Y. Zhao, S. Yao, D. Liu, H. Shao, and S. Liu, "Greenroute: A generalizable fuel-saving vehicular navigation service," in *2019 IEEE International Conference on Autonomic Computing (ICAC)*, 2019, pp. 1–10.
- [6] H. Wu and S. Malipeddi, "Influential factors for severe traffic crashes," in *Proceedings of 2011 IEEE International Conference on Vehicular Electronics and Safety*, 2011, pp. 71–75.
- [7] E.-H. Choi, "Crash factors in intersection-related crashes: An on-scene perspective," 2010.
- [8] E. A. Bellis and J. Page, "National motor vehicle crash causation survey (nmvccs) sas analytical users manual," 2008.
- [9] L. Chen and C. Englund, "Cooperative intersection management: A survey," *IEEE Transactions on Intelligent Transportation Systems*, vol. 17, no. 2, pp. 570–586, 2016.
- [10] D. González, J. Pérez, V. Milanés, and F. Nashashibi, "A review of motion planning techniques for automated vehicles," *IEEE Transactions on Intelligent Transportation Systems*, vol. 17, no. 4, pp. 1135–1145, 2016.
- [11] J. Lee and B. Park, "Development and evaluation of a cooperative vehicle intersection control algorithm under the connected vehicles environment," *IEEE Transactions on Intelligent Transportation Systems*, vol. 13, no. 1, pp. 81–90, 2012.
- [12] M. A. S. Kamal, J.-i. Imura, T. Hayakawa, A. Ohata, and K. Aihara, "A vehicle-intersection coordination scheme for smooth flows of traffic without using traffic lights," *IEEE Transactions on Intelligent Transportation Systems*, vol. 16, no. 3, pp. 1136–1147, 2015.
- [13] S. Li, K. Shu, Y. Zhou, D. Cao, and B. Ran, "Cooperative critical turning point-based decision-making and planning for cavih intersection management system," *IEEE Transactions on Intelligent Transportation Systems*, vol. 23, no. 8, pp. 11 062–11 072, 2022.
- [14] R. Hult, G. R. Campos, E. Steinmetz, L. Hammarstrand, P. Falcone, and H. Wymeersch, "Coordination of cooperative autonomous vehicles: Toward safer and more efficient road transportation," *IEEE Signal Processing Magazine*, vol. 33, no. 6, pp. 74–84, Nov 2016.
- [15] G. Rodrigues de Campos, P. Falcone, R. Hult, H. Wymeersch, and J. Sjöberg, "Traffic coordination at road intersections: Autonomous decision-making algorithms using model-based heuristics," *IEEE Intelligent Transportation Systems Magazine*, vol. 9, no. 1, pp. 8–21, 2017.
- [16] Y. Mo, M. Wang, T. Zhang, and Q. Zhang, "Autonomous cooperative vehicle coordination at road intersections," in *2018 IEEE International Conference on Communication Systems (ICCS)*, 2018, pp. 192–197.
- [17] C. Liu, Y. Mo, B. Gao, and T. Zhang, "Low complexity coordination strategies at multi-lane intersections," in *2019 IEEE Globecom Workshops (GC Wkshps)*, 2019, pp. 1–6.
- [18] C. Liu, Y. Zhang, T. Zhang, X. Wu, L. Gao, and Q. Zhang, "High throughput vehicle coordination strategies at road intersections," *IEEE Transactions on Vehicular Technology*, vol. 69, no. 12, pp. 14 341–14 354, 2020.
- [19] M. Wang, T. Zhang, L. Gao, and Q. Zhang, "High throughput dynamic vehicle coordination for intersection ground traffic," in *2018 IEEE 88th Vehicular Technology Conference (VTC-Fall)*, 2018, pp. 1–6.
- [20] X. Pan, B. Chen, S. Timotheou, and S. A. Evangelou, "A convex optimal control framework for autonomous vehicle intersection crossing," *IEEE Transactions on Intelligent Transportation Systems*, vol. 24, no. 1, pp. 163–177, 2023.
- [21] H. Fan, F. Zhu, C. Liu, L. Zhang, L. Zhuang, D. Li, W. Zhu, J. Hu, H. Li, and Q. Kong, "Baidu apollo EM motion planner," *CoRR*, vol. abs/1807.08048, 2018. [Online]. Available: <http://arxiv.org/abs/1807.08048>
- [22] Y. Zhang, G. Chen, and T. Zhang, "Intelligent intersection coordination and trajectory optimization for autonomous vehicles," in *2021 IEEE International Conference on Autonomous Systems (ICAS)*, 2021, pp. 1–6.
- [23] F. Perronnet, J. Buisson, A. Lombard, A. Abbas-Turki, M. Ahmane, and A. El Moudni, "Deadlock prevention of self-driving vehicles in a network of intersections," *IEEE Transactions on Intelligent Transportation Systems*, vol. 20, no. 11, pp. 4219–4233, 2019.
- [24] J. Luo, T. Zhang, R. Hao, D. Li, C. Chen, Z. Na, and Q. Zhang, "Real-time cooperative vehicle coordination at unsignalized road intersections," *arXiv e-prints*, p. arXiv:2205.01278, May 2022.
- [25] J. Kong, M. Pfeiffer, G. Schildbach, and F. Borrelli, "Kinematic and dynamic vehicle models for autonomous driving control design," in *2015 IEEE Intelligent Vehicles Symposium (IV)*, 2015, pp. 1094–1099.
- [26] T. Liang, T. Zhang, J. Yang, D. Feng, and Q. Zhang, "UAV-Aided positioning systems for ground devices: Fundamental limits and algorithms," *IEEE Internet of Things Journal*, vol. 9, no. 15, pp. 13 470–13 485, 2022.
- [27] H. Li, M. Tsukada, F. Nashashibi, and M. Parent, "Multivehicle cooperative local mapping: A methodology based on occupancy grid map merging," *IEEE Transactions on Intelligent Transportation Systems*, vol. 15, no. 5, pp. 2089–2100, 2014.
- [28] J. Horst and A. Barbera, "Trajectory generation for an on-road autonomous vehicle," *Proc Spie*, vol. 6230, p. 82, 2006.
- [29] M. Werling, J. Ziegler, S. Kammel, and S. Thrun, "Optimal trajectory generation for dynamic street scenarios in a frenet frame," *2010 IEEE International Conference on Robotics and Automation*, pp. 987–993, 2010.
- [30] D. Mellinger and V. Kumar, "Minimum snap trajectory generation and control for quadrotors," in *2011 IEEE International Conference on Robotics and Automation*, 2011, pp. 2520–2525.

- [31] Neely and J. Michael, "Stochastic network optimization with application to communication and queueing systems," *Synthesis Lectures on Communication Networks*, vol. 3, no. 1, p. 211, 2010.
- [32] X. Zhou, Z. Wang, H. Ye, C. Xu, and F. Gao, "Ego-planner: An esdf-free gradient-based local planner for quadrotors," *IEEE Robotics and Automation Letters*, vol. 6, no. 2, pp. 478–485, 2021.
- [33] V. Usenko, L. von Stumberg, A. Pangercic, and D. Cremers, "Real-time trajectory replanning for mavs using uniform b-splines and a 3d circular buffer," in *2017 IEEE/RSJ International Conference on Intelligent Robots and Systems (IROS)*, 2017, pp. 215–222.
- [34] H. Zhao, J. Gao, T. Lan, C. Sun, B. Sapp, B. Varadarajan, Y. Shen, Y. Shen, Y. Chai, C. Schmid, C. Li, and D. Anguelov, "TNT: Target-driveN trajectory prediction," *arXiv e-prints*, p. arXiv:2008.08294, Aug. 2020.
- [35] P. T. Boggs and R. H. Byrd, "Adaptive, limited-memory BFGS algorithms for unconstrained optimization," *SIAM Journal on Optimization*, vol. 29, no. 2, pp. 1282–1299, 2019. [Online]. Available: <https://doi.org/10.1137/16M1065100>
- [36] J. Wang, Y. Yan, K. Zhang, Y. Chen, M. Cao, and G. Yin, "Path planning on large curvature roads using driver-vehicle-road system based on the kinematic vehicle model," *IEEE Transactions on Vehicular Technology*, vol. 71, no. 1, pp. 311–325, 2022.
- [37] M. Quigley, B. P. Gerkey, K. Conley, J. Faust, and A. Y. Ng, "Ros: An open-source robot operating system," 2009.